Jawad FAIZ[1], Mehdi MANOOCHEHRY[2], Ghazanfar SHAHGHOLIAN[2]

University of Tehran (1), Islamic Azad University (2)

Performance Improvement of Permanent Magnet Linear Synchronous Motor Drive using Space Vector Modulated-Direct Thrust Force Control

Abstract. *This paper proposes a space vector modulation (SVM) direct thrust force control (DFC) concept to minimize the ripples of the electromagnetic thrust force and flux-linkage, and fix the switching frequency in a conventional DFC system for permanent magnet linear synchronous motors. A special method called symmetrical SVM is applied to achieve a high performance drive. Simulation results show that the proposed SVM-DFC can improve the steady-state performance considerably while keeping the dynamic performance of the conventional DFC.*

Streszczenie. *W artykule zaproponowano wykorzystanie modulacji wektora przestrzennego SVM i bezpośrednie sterowanie siłą ciągu DFC do minimalizacji zafalowań siły ciągu w synchronicznym silniku z magnesami trwałymi. Rezuyltaty symulacji pokazały że zaproponowany system SVM-DFC pozwla na poprawę właściwości silnika w stanie ustalonym przy właściwościach dynamicznych nie gorszych niż w układach konwencjonalnych. (**Poprawa parametrów liniowego silnika synchronicznego z magnesami trwałymi przy użyciu metod SVM i TFC**)*

Keywords: PMLSM, DFC, Symmetrical SVM, DFC-SVM.
Słowa kluczowe: liniowy silnik synchroniczny, SVM, DFC.

Introduction

Ever increasing extensive application of linear motors in transportation systems, elevators and other linear move result in a wide investigation of these types of electrical motors. Advantages of permanent magnet linear synchronous motor (PMLSM) compared to other linear motors lead to wide application of PMLSM in industrial systems particularly where a precise move is vital. The most important advantages of PMLSM include high efficiency, appropriate power factor, low friction, high axial force density and low heat losses [1-4]. To design a secure drive system for PMLSM, a control system having an appropriate performance is required to be able to compensate the parameters variations, load disturbance, friction, uncertain dynamics and difficulty of using conventional gear systems. Direct torque control (DTC) method was introduced in 1986 for controlling rotating AC motors [5]. Many advantages of this control method including simplicity, absence of speed sensors and current regulators, and needless complicated and many transformations (which required in vector control technique) and particularly lower sensitivity toward system parameters variations results in the wide application of the method in rotating AC electrical machines [6-8]. These advantages lead to the extension of the method to its counterparts-linear electrical motors particularly PMLSM. In this case the axial thrust force is directly controlled and the method is called direct thrust force control (DFC) [9-12].

In spite of many advantages of DTC and DFC methods, they have a number of drawbacks. One of these problems, which is more significant in linear motors due to their structure, is high ripples in thrust force and flux-linkage of the motor. Also switching frequency is not constant in this method. Many techniques have been so far implemented to solve these problems in DTC method applied to rotating AC motors. However, there are a few techniques to solve the similar problems in linear motors, so a wider research in this area is required.

Some techniques to improve DTC or DFC are reviewed in the following part. A new integrator structure has been introduced for flux estimation in [9], and a new look-up table has been also given to reduce the torque or force ripples. In spite of implementing this system, determining controller coefficients by genetic algorithm and building a new integrator, it is practically difficult to use it. Sliding mode control can be used as a method to reduce the force ripples in DFC method [11, 13]. Although simulation results show the merit of the method, the method depends on the parameters of the motor and it is difficult to obtain an appropriate Lyapanov function. Fuzzy control can be implemented to overcome the DFC method drawbacks. This method is a new and suitable one, however design of this method requires an experienced designer. To evolve the accuracy of the Fuzzy method, a large number of cases must be processed which needs huge computations and an appropriate processor and this leads to a costly system. In [14], considering limited number of states in DTC method for three phase system, enhancement of the phase number has been proposed as solution. This method has been implemented for a prototype motor, but substituting this motor with a three phase motor in industry is not economical.

DFC-SVM method consists of a DFC control system in which SVM is used for switching the drive. In this method, a combination of a three-phase inverter voltage vectors is utilized. Thus, a continuous space is used to generate voltage instead of discrete space with 6 basic voltage vector states. Consequently, this control system will be efficient in the reduction of the distortion of the drive system parameters such as developed electromagnetic force, flux-linkage and speed of the motor. Also the nature of this switching method results in fixing the switching frequency [15].

In the present paper two basic DFC and SVM-DFC are used for PMLSM. In section 2 an appropriate modeling for motor is introduced. Section 3 describes how DFC method is designed and implemented in PMLSM. In section 4, SVM method is presented and proposed system (SVM-DFC) is introduced and used in PMLSM. Simulation results and their comparisons are given in section 5. The paper is concluded in section 6.

Modeling of PMLSM

The following assumptions are considered in PMLSM:

1. Fundamental component is considered due to sinusoidal distribution of magnetic fields.
2. Magnetic saturation is ignored.
3. Hysteresis losses and leakage flux are neglected.
4. There is a damping winding in the primary winding of the motor.

The model is proposed in the rotor d-q system and therefore transformations between the axes are required. At this end, first abc voltage equations of stator are transformed into two-axes d-q equations in the rotor:

$$V_d = Ri_d + \frac{d\psi_d}{dt} - \omega\psi_q \quad (1)$$

$$V_q = Ri_q + \frac{d\psi_q}{dt} + \omega\psi_d \quad (2)$$

$$\psi_d = L_{ad}i_d + \psi_{PM} \quad (3)$$

$$\psi_q = L_{aq}i_q \quad (4)$$

The axial force (F_M) is as follows:

$$F_M = \frac{3}{2}P\frac{\pi}{\tau}\left[\psi_{PM} + (L_{ad} - L_{aq})i_d\right]i_q \quad (5)$$

And mechanical equations are:

$$M\dot{v} = F_M - F_L - Bv - F_{end-effect} \quad (6)$$

$$F_{end-effect} = K_{end}F_{Thrust} \quad (7)$$

End-effect is the effect of the limited length of the mover in linear motors. Generally it is difficult to model the end-effect with exact mathematical equations. In practice many researchers use multiplying coefficient or function which takes into account the thrust reduction due to the end-effect [18]. In this paper the value of end-effect coefficient is determined according to equation (7).

Taking into account the transformation between the systems and the above equations the modeling of PMLSM is as shown in Fig. 4. Sub-systems due to the voltage equations have been presented in Fig. 1 and Fig. 2, and mechanical sub-system has been shown in Fig. 3.

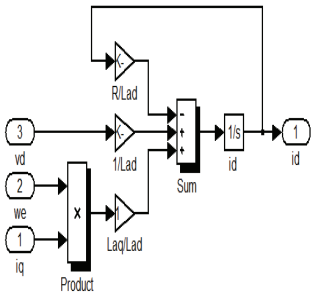

Fig. 1. Driving PMLSM d-axis current

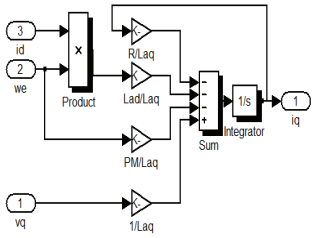

Fig. 2. Driving PMLSM q-axis current

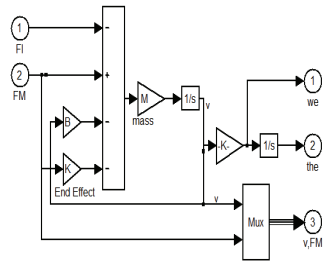

Fig. 3. Motion mechanical equation in PMLSM

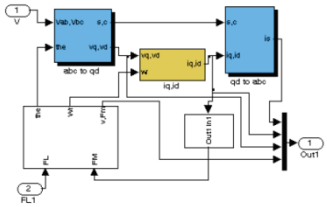

Fig. 4. Block diagram of PMLSM

Direct trust force control in PMLSM

DFC in linear motors determines the optimal value of the voltage based on the flux-linkage and electromagnetic force. This value is obtained from lookup table that is introduced in table.1. In DFC method the motor is supplied by a three-phase inverter. It generates six non-zero voltage vectors and two zero voltage vectors based on eight states. Fig. 5 shows the different states of the voltage vector with their relevant regions (P_n) [16].

This control system operates based on the direct control of the flux-linkage and electromagnetic force of the motor. The actual value and reference value are compared and the error enters to the hysteresis controllers, then the output of these controllers select the most suitable and effective voltage vector from the look-up table. The basic DFC control system has been shown in Fig. 6. Flux-linkage and electromagnetic force of the motor have been obtained approximately. It is possible to calculate the flux of motor from the motor voltages (u_{sa}, u_{sb}) and currents (i_{sa}, i_{sb}) in the stator stationary two-axes system using an integrator as follows:

$$\psi_D = \int(V_D - R_s.i_D)dt \quad (8)$$

$$\psi_Q = \int(V_Q - R_s.i_Q)dt \quad (9)$$

The amplitude of stator flux-linkage is determined as follows:

$$|\psi_s| = \sqrt{(\psi_D)^2 + (\psi_Q)^2} \quad (10)$$

Also the motor angle which shows the flux vectors positions is obtained as follows:

$$\theta = \mathrm{Tan}^{-1}\left(\frac{\psi_Q}{\psi_D}\right) \quad (11)$$

This angle is used to determine the effective region. The developed electromagnetic force of the motor is obtained as follows:

$$F = \frac{3}{2}P\frac{\pi}{\tau}(\psi_D i_Q - \psi_Q i_D) \quad (12)$$

In the above equations the major advantage of DFC method, compared to other control method, is the existence of the stator resistance as unique parameter.

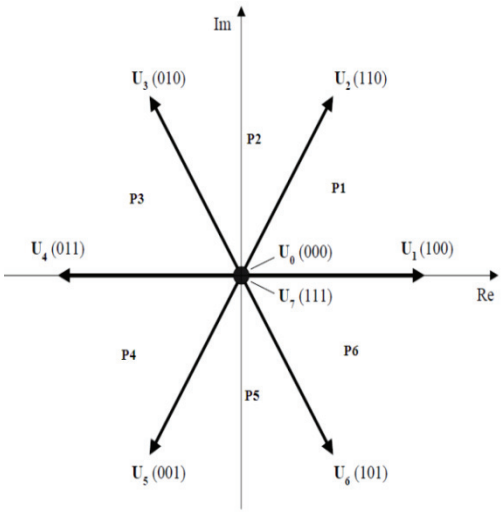

Fig. 5. Inverter voltage vectors with their six sates

Table 1. Lookup table

O_φ	O_f	P1	P2	P3	P4	P5	P6
1	1	U_2	U_3	U_4	U_5	U_6	U_1
	0	U_0	U_7	U_0	U_7	U_0	U_7
	-1	U_6	U_1	U_2	U_3	U_4	U_5
0	1	U_3	U_4	U_5	U_6	U_1	U_2
	0	U_0	U_7	U_0	U_7	U_0	U_7
	-1	U_5	U_6	U_1	U_2	U_3	U_4

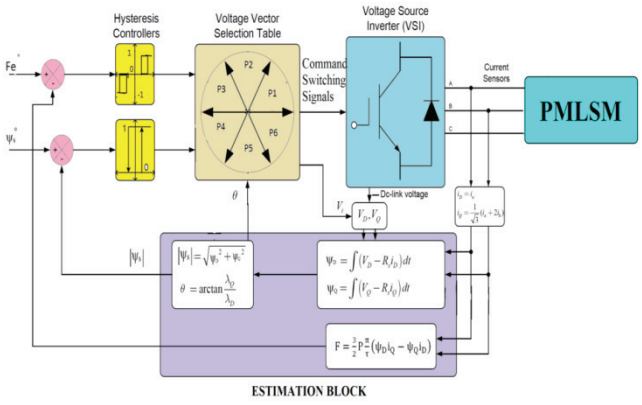

Fig. 6. Basic DFC control system for PMLSM

Direct trust force control using space vector modulation method (SVM-DFC)

As shown in section 6, thrust force and flux-linkage using the basic DFC method have relatively large ripple. In addition, varying switching frequency increases the losses, distortion, and low-order harmonics in the motor current. The main reason for these problems is the structure of the basic DFC control system. Since hysteresis controllers and look-up table are used in the basic DFC method, there is a type of discontinuity in the applied voltage vectors because only six non-zero voltage vectors are used which leads to distortion. Also this control system generates the switches commands directly, switching frequency is variable. To remove these defects, space vector modulation (SVM) has been recommended [15]. This method can considerably decrease the electromagnetic force and flux-linkage ripples and fix the switching frequency substituting discontinues voltage vector space selection with continues space. In this method, a PI controller is used in the place of the hysteresis controllers; the look-up table is replaced by SVM voltage generating block. DFC-SVM control system has been shown in Fig. 7.

A. Space voltage vector generation

To generate the reference voltage V_{sref}, there need two voltage vector components (V_{sa}, V_{sb}). To obtain the stator flux-linkage error ($d\psi_s$) the following equations are used referring to Fig. 8:

$$F = \frac{3P}{2L_s}|\psi_s||\psi_{PM}|\sin\delta \quad (13)$$

$$d\psi_{sa} = \psi_{sr}.\cos(\theta + d\delta) - |\psi_s|.\cos(\theta) \quad (14)$$

$$d\psi_{sb} = \psi_{sr}.\sin(\theta + d\delta) - |\psi_s|.\sin(\theta) \quad (15)$$

$$V_{sa} = \frac{d\psi_{sa}}{T_z} + R_s.i_{sa} \quad (16)$$

$$V_{sb} = \frac{d\psi_{sb}}{T_z} + R_s.i_{sb} \quad (17)$$

where ψ_{sr} is the reference flux-linkage, ψ_{PM} is the rotor flux-linkage, $d\delta$ is the angle difference between the reference flux and stator resultant flux ψ_s and T_z is the sampling time. $d\delta$ is obtained using a PI controller based on (13). Switching signal is generated in three stage.

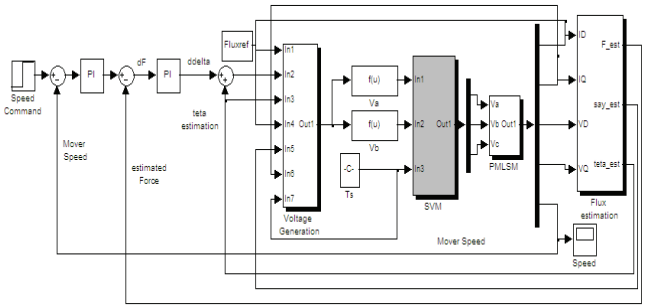

Fig. 7. DFC-SVM control system for PMLSM

B. Reference Signal Generation

The generated voltage vector components using (16) and (17), the magnitude ($|V_{sref}|$) and angle (α) of the reference voltage vector are determined as follows:

$$|V_{sref}| = \sqrt{(V_{sa})^2 + (V_{sb})^2} \quad (18)$$

$$\alpha = \tan^{-1}\left(\frac{V_{sb}}{V_{sa}}\right) \quad (19)$$

This vector has been presented in Fig. 9.

C. Time Estimation for Applying Basic Voltage Vectors

Considering the continuity of the method, the reference voltage vector is generated from eight basic vectors by inverter. In any sampling period, two non-zero voltage vectors and one zero-voltage vector are required considering the reference vector position. Considering its region (n), the time of applying any basic vector is obtained as follows:

$$T_1 = \frac{\sqrt{3}.T_z.|\bar{V}_{ref}|}{V_{dc}}\left[\sin\left(\frac{n\pi}{3} - \alpha\right)\right] \quad (20)$$

$$T_2 = \frac{\sqrt{3}.T_z.|\bar{V}_{ref}|}{V_{dc}}\left[\sin\left(\alpha - \frac{n-1}{3}\pi\right)\right] \quad (21)$$

$$T_0 = T_z - T_1 - T_2 \quad (22)$$

where $T_z=1/f_s$. Fig. 9 shows the procedure for applying these times in the first region.

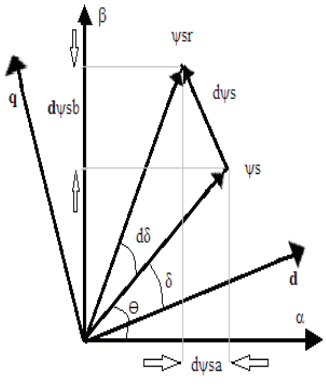

Fig. 8. Stator flux diagram and its errors

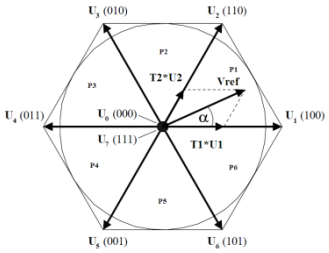

Fig. 9. Determination of time durations using reference voltage vector and basic vectors in the first region

D. Generating Switches Command Signal

There are various methods for generating the switches command signal which differ according to the ordering of the zero-voltage vectors. To reduce the THD a symmetrical type is used here [17]. By applying this method, switching

signals are provided as Table 2. This table shows the command signals of three upper switches of each leg of the inverter. To prevent the short-circuit, the command signal of the three lower switches are opposite to that of the upper switches.

Simulation results and comparison between two systems

The introduced systems are simulated using MATLAB SIMULINC. System introduced in Fig. 6 is used to simulate the basic DFC drive and system introduced in Fig. 7 is utilized to simulate SVM-DFC drive. The sampling time is taken to be T_z=400 μs. The PI controller has been adjusted using trial and error routine. To apply the methods, the PMLSM with parameters given in Table 3 and according to the model introduced in section 2 are simulated. Fig. 10 shows the speed characteristics of two systems. Fig. 10a presents the motor speed using the basic DFC method. It is clear that there is a steady-state error in the speed response and also distortion in the speed characteristic. The settling time is 4.9s. Fig. 10b shows the corresponding characteristic using SVM-DFC method. Application of this method results in the zero steady-state error. The settling time is 1.8s which is considerably shorter than 4.9 s (previous case). Fig. 11 presents the distortion level using the two methods. It is clear that the distortion level has been reduced from 0.3 m/s to 0.1 m/s.

Fig. 12 shows the electromagnetic force of the motor in two cases. As expected, the distortion of the force in SVM-DFC is lower. Table 4 summarizes the results of applying two methods.

To investigate the performance of the drive systems, the impact of varying the reference speed and its response tracking are considered. Fig. 13 shows speed tracking in both systems. Although both methods follow the reference speed, higher steady-state error and distortion are visible in Fig. 13a. These indexes have been improved in Fig. 13b. In addition, transient period in the SVM-DFC is shorter and speed waveform is flatter. Another important factor in the study of the drive system performance is the impact of the load and its fluctuations upon the output response.

Table 2. Switching algorithm for symmetrical SVM

Sector	Command signal
1	$V_0 \rightarrow V_1 \rightarrow V_2 \rightarrow V_7 \rightarrow V_2 \rightarrow V_1 \rightarrow V_0$
	$S1=T_1/2+T_2/2+T_0/2+T_2/2+T_1/2$
	$S3=T_2/2+T_0/2+T_2/2$
	$S5=T_0/2$
2	$V_0 \rightarrow V_3 \rightarrow V_2 \rightarrow V_7 \rightarrow V_2 \rightarrow V_3 \rightarrow V_0$
	$S1= T_2/2+T_0/2+T_2/2$
	$S3= T_1/2+T_2/2+T_0/2+T_2/2+T_1/2$
	$S5= T_0/2$
3	$V_0 \rightarrow V_3 \rightarrow V_4 \rightarrow V_7 \rightarrow V_4 \rightarrow V_3 \rightarrow V_0$
	$S1= T_0/2$
	$S3= T_1/2+T_2/2+T_0/2+T_2/2+T_1/2$
	$S5= T_2/2+T_0/2+T_2/2$
4	$V_0 \rightarrow V_5 \rightarrow V_4 \rightarrow V_7 \rightarrow V_4 \rightarrow V_5 \rightarrow V_0$
	$S1= T_0/2$
	$S3= T_2/2+T_0/2+T_2/2$
	$S5= T_1/2+T_2/2+T_0/2+T_2/2+T_1/2$
5	$V_0 \rightarrow V_5 \rightarrow V_6 \rightarrow V_7 \rightarrow V_6 \rightarrow V_5 \rightarrow V_0$
	$S1= T_2/2+T_0/2+T_2/2$
	$S3= T_0/2$
	$S5= T_1/2+T_2/2+T_0/2+T_2/2+T_1/2$
6	$V_0 \rightarrow V_1 \rightarrow V_6 \rightarrow V_7 \rightarrow V_6 \rightarrow V_1 \rightarrow V_0$
	$S1= T_1/2+T_2/2+T_0/2+T_2/2+T_1/2$
	$S3= T_0/2$
	$S5= T_2/2+T_0/2+T_2/2$

Fig. 14 exhibits the influence of the varying load on the speed of the motor. According to Fig. 14a, load changing in the basic DFC drive leads to speed distortion. But in the SVM-DFC drive, system is robust against load changes (Fig. 14b) and there is no change in transient period of its final value. Also Fig.15 shows systems load tracking. According to the figures, there is more desirable load tracking in SVM-DFC compared to basic DFC. In basic DFC system in addition to large ripple in steady-state durations, load changing leads to high thrust force ripples in long transient times. Finally flux-linkage schemes of the motor using the two methods are shown in Fig. 16. It shows that the flux distortion during the transient period has been decreased in SVM-DFC system.

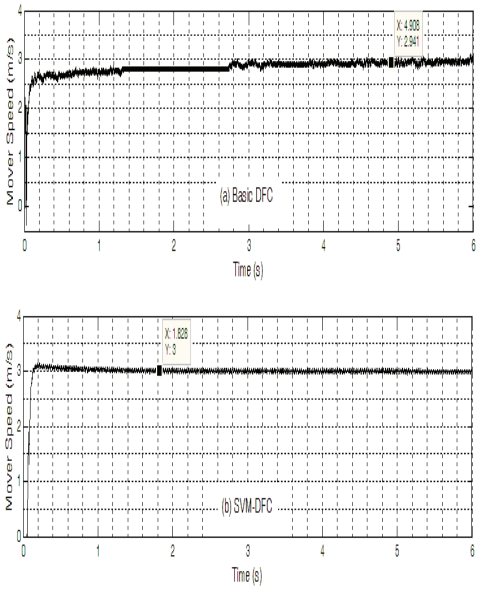

Fig. 10. Motor speed with reference speed equal to 3 m/s: (a) basic DFC method and (b) SVM-DFC method

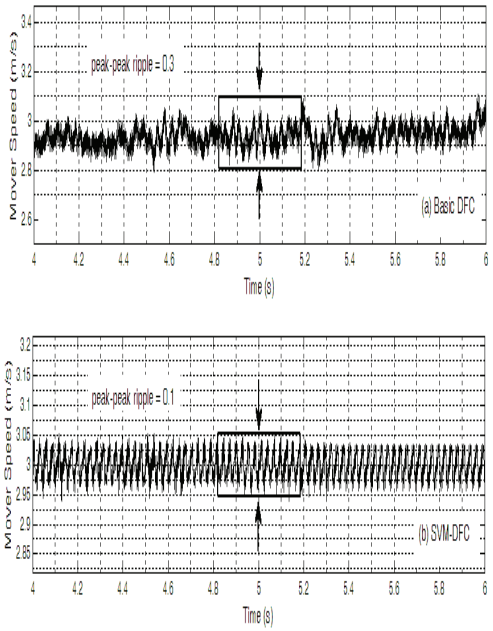

Fig. 11. Motor speed distortion: (a) basic DFC method and (b) SVM-DFC method

Conclusion

The basic DFC method has a number of drawbacks including varying switching frequency, high distortion in electromagnetic force and flux of the PMLSM and also

motor speed characteristic, therefore combination of SVM and DFC methods were applied in this paper. Considering the structure of the modulation, the switching frequency is fixed and distortion of the control system characteristics such as electromagnetic force and flux is decreased. As shown in Table 4, the speed distortion more than 60% and force more than 30% are reduced. Also the settling time of speed improves 62% and steady-state error becomes zero.

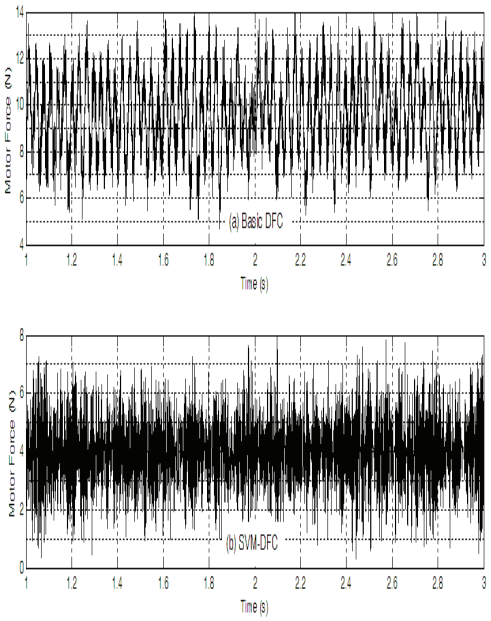

Fig. 12. Motor electromagnetic force: (top) basic DFC method and (bottom) SVM-DFC method

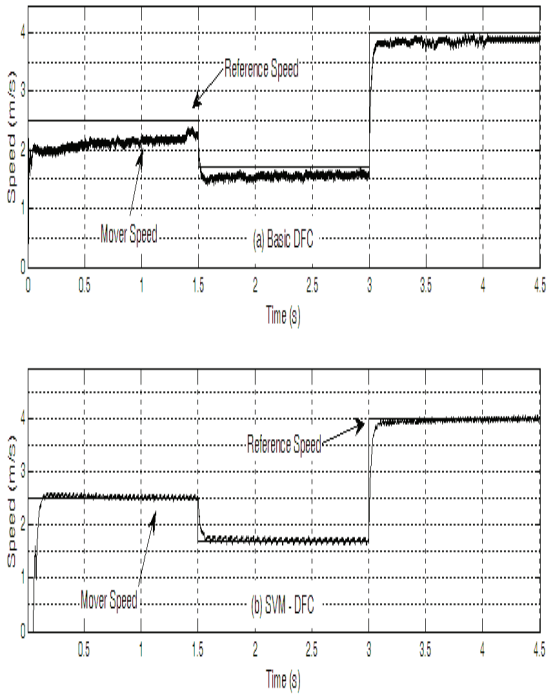

Fig. 13. Motor speed tracking: (top) basic DFC method and (bottom) SVM-DFC method

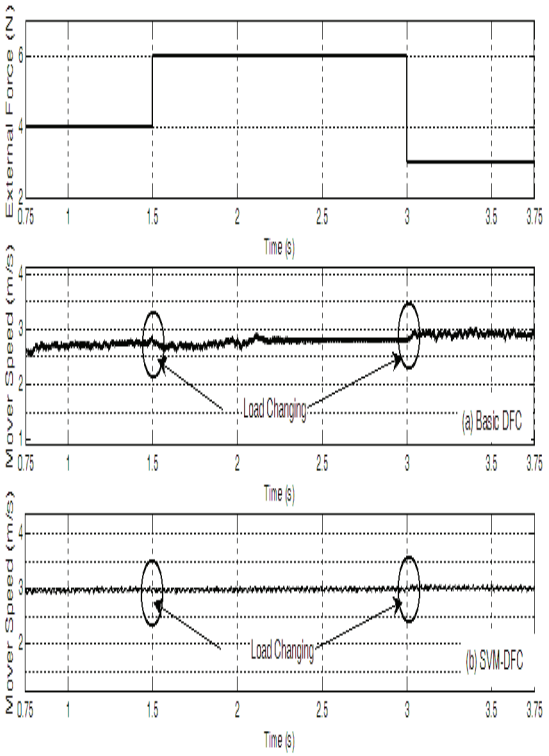

Fig. 14. Motor speed response during load changing: (middle) basic DFC method and (bottom) SVM-DFC method

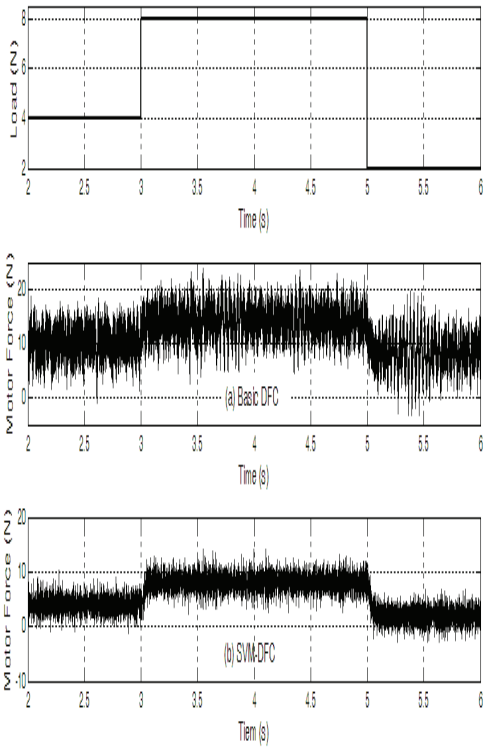

Fig. 15. Thrust force tracking: (middle) basic DFC method and (bottom) SVM-DFC method

Table. 3. Specifications of the proposed PMLSM

Parameter	Value
Pole pairs	1
Pole pitch	42 m
Stator resistance	2 Ω
Inductances of dq axes	2.63 mH
PM flux	0.17 Wb
Motor damping coefficient	9.91 Ns/m
DC voltage	173.2 V

Table 4. Comparison of indexes of two drive systems at reference speed equal to 3 m/s and external force of 4 N

Type of drive	Basic DFC	SVM-DFC
Speed steady-state error	0.06	0
Settling time (s)	4.8	1.8
Speed distortion level (m/s)	0.3	0.1
Motor force distortion level (N)	9	6

Robustness of the control system against load changes and reference speed tracking in two systems were studied. Distortion of the speed due to the load variation diminishes and steady-state error in the speed tracking tends to zero. Consequently, the combined SVM-DFC control method can utilize the DFC control method advantages and reduces its drawbacks considerably.

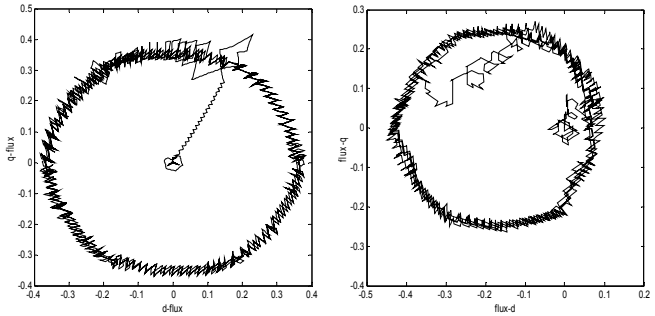

(a) (b)

Fig. 16. Motor flux-linkage variations: (a) basic DFC method and (b) SVM-DFC method

List of symbols

Symbol	Definition	Unit
i_d, i_q	d-q axis currents	A
V_d, V_q	d-q axis voltages	V
V_{sa}, V_{sb}	D-Q axis voltage	V
L_{ad}, L_{aq}	d-q axis inductances	H
R	Winding resistance	Ω
M	Mover mass	kg
B	Viscous friction coefficient	Ns/m
τ	Pole pitch	m
ψ_{PM}	Permanent magnet flux	Wb
F_L	Load force	N
ω_r	Angular speed (=πV/τ)	rad/s
v	Linear speed	m/s
K_{end}	End Effect coefficient	
O_f	Force hysteresis output	
Oψ	Flux hysteresis output	
P	PMLSM pole pairs	
θ	Motor angle	
δ	Angle between PM and stator Flux	

REFERENCES

[1] Cheng B., Tesch T.R., Torque feed forward control technique for permanent-magnet synchronous motor", IEEE Trans. on Ind. Elec., 57(2010), No. 3, 969-974.

[2] Huang Y.S., Sung C.C., Yu C.S., Reduced order fuzzy sliding mode control for linear synchronous motor systems, IEEE/ICIT, March 2010, 392-397, Vi a del Mar,.

[3] Huang Y.S., Sung C.C., Shih Y.T., Simulation of a robust fuzzy controller for linear synchronous motor systems, IEEE/SMC, 2008, 2001-2006.

[4] Huang Y.S., Sung C.C., Function-based controller for linear motor control system, IEEE Trans. on Ind. Ele., 57 (2010), No. 3, 1096-1105.

[5] Isao T.,Toshihiko N., A new quick-response and high-efficiency control strategy of an induction motor, IEEE Trans. Ind. Appl., 22 (1986), No. 5, 820-827.

[6] Depenbrock M., Direct self control (DSC) of inverter-fed induction machine, IEEE Trans. Pow. Elec., 3 (1988), No. 4, 420-429.

[7] Baader U., Depenbrock M., Gierse G., Direct self control (DSC) of inverter-fed induction machine: A basis for speed control without speed measurement, IEEE Trans. Ind. Appl., 28 (1992), No. 3, 581-588.

[8] Altonen M., Tiitinen P., Lalu J., Heikkila S., "irect torque control of AC motor drives", Abb Rewiew, (1995), 19-24.

[9] Sung C., Huang Y., Based on direct thrust control for linear synchronous motor systems, IEEE Trans. Ind. Elec., 56 (2009), No. 5, 1629-1639.

[10] Abroshan M., Malekian K., Milimonfared J., Varmiab B.A., An optimal direct thrust force control for interior permanent magnet linear synchronous motors incorporating field weakening, IEEE/SPEEDAM, June 2008, Ischia, 130-135,.

[11] Lirong G., Junyou Y., Jiefan C., Direct thrust control approach using adaptive variable structure for permanent magnet linear synchronous motor, IEEE/ICCA, 2007, 2217-2220.

[12] Huang Y., Sung C., Shih Y., Simulation of a robust fuzzy cont-roller for linear synchronous motor systems", IEEE/ICSMC, Singapore, Oct. 2008, 2001-2006,.

[13] Lirong G., Junyou Y., Jiefan C., Direct thrust control approach using adaptive variable structure for permanent magnet linear synchronous motor, IEEE/ICCA, Guangzhou, May/June 2007, 2217-2220,.

[14] Parsa L., Performance improvement of permanent magnet AC motors, PhD Thesis, Texas A&M University, 2005.

[15] Neacsu D.O., Space vector modulation - An introduction", IEEE/IECON, 2001,1583-1592.

[16] Jiefan C., Chengyuan W., Junyou Y., Lifeng L., Analysis of direct thrust force control for permanent magnet linear synchronous motor, IEEE/WCICA, 5, June 2004, 4418-4421.

[17] Zelechowski M., Space vector modulated-direct torque controlled (DTC-SVM) inverter-fed induction motor drive, PhD Thesis, Warsaw University of Tech, Poland, 2005.

[18] Ponomarev P., Control of permanent magnet linear synchronous motor in motion application, M.Sc Thesis, Lappeenranta University of Tech, 2009.

Authors: *Prof. Jawad Faiz is with Center of Excellence on Applied Electromagnetic Systems, School of Electrical and Computer Engineering, University College of Engineering, University of Tehran,Tehran, Iran, Email{ jfaiz@ut.ac.ir. Mehdi Manoochehry and Dr. Ghazanfar Shahgholian are with Department of Electrical Engineering, Islamic Azad University, Najafabad Branch, Isfahan, Iran.*